Available online at www.sciencedirect.com

SciVerse ScienceDirect

Physics Procedia 37 (2012) 838 – 843

Physics Procedia

TIPP 2011 – Technology and Instrumentation in Particle Physics 2011

Design of Punch-Through Protection of Silicon Microstrip Detector against Accelerator Beam Splash

K. Hara[a*], N. Hamasaki[a], Y. Takahashi[a], S. Mitsui[b] Y. Ikegami[c], Y. Takubo[c], S. Terada[c], Y. Unno[c]

[a]*IPAS, University of Tsukuba, Tennodai 1-1-1, Tsukuba, 305-8571 Ibaraki, Japan*
[b]*Graduate University for Advanced Studies (Soken-Dai), Oho 1-1, Tsukuba, 305-0801 Ibaraki, Japan*
[c]*INPS, High Energy Accelerator Research Org.(KEK), Oho 1-1, Tsukuba, 305-0801 Ibaraki, Japan*

Abstract

In experiments at high intensity accelerators such as the LHC and its planned upgrade, HL-LHC, the silicon microstrip detector should be designed to survive against possible beam loss that may create large amount of signal charges in short period. We are designing a built-in protection structure based on a punch through mechanism for the p-bulk n^+-readout sensors under development for the HL-LHC. The performance is evaluated by applying DC voltages and also by using a pulsed infrared laser to generate a large amount of current. The latter test provides the time information of the protection system.

© 2012 Published by Elsevier B.V. Selection and/or peer review under responsibility of the organizing committee for TIPP 11.

Keywords: microstrip sensor; punch-through; strip protection; beam loss;

1. Introduction

The Large-Hadron Collider (LHC) under operation at CERN will collide the proton bunches (10^{11} protons/bunch) at 40 MHz at its design. Such high intensity beams are the key to explorer the nature of particle physics to depth. At an incident of beam loss happening in the detector area, a beam aborting system will be triggered but the activation takes typically 1 ms. Therefore several times 10^{12} protons could be splashed over the detector area in the worst case.

The ATLAS SCT employs the n-bulk and AC-coupled p-readout microstrip sensors (p^+-in-n sensors). A protection mechanism against such beam splashes is implemented on this senor by extending the p^+-

* Email: hara@hep.px.tsukuba.ac.jp

1875-3892 © 2012 Published by Elsevier B.V. Selection and/or peer review under responsibility of the organizing committee for TIPP 11.
doi:10.1016/j.phpro.2012.02.427

implant ends close as much as 5 μm [1][2] to the bias-ring to activate the punch-through (PT). A study [3] points out that even under such protection the strip could be damaged by an extremely intense beam splash due mainly to the finite implant resistance. Fig. 1(a) shows a hole was formed on an SCT sensor operated at 500 V when a charge equivalent to 10^8 minimum ionizing particles (mips) was injected in an area 10 μm square aside from the electrode. This sensor for example went un-operational for failure of sustaining the bias voltage. Other effects were also observed such as several strips at neighbours or whole chip started to show substantial increase in noise. The studied case should be regarded as quite rare at the LHC since the protons are expected to splash in wider area, but the study suggests that an efficient protection design is mandatory to minimize the risk of damage.

A new type of microstrip sensors is designed utilizing p-bulk wafers [4] for the planned High Luminosity LHC. As schematically explained in Fig. 1(b), protection of the insulator from breaking is achieved by low impedance between the implant and the bias-ring, which is realized by a punch-through mechanism, or PTP [5]. One difficulty in this design is the existence of the p-stop. The p-stop, which is required for p-bulk sensors for preventing mobile electrons accumulated at the surface to degrade the strip isolation, acts as a punch-through blocker at the same time. We examined the PTP for various configurations of the strip ends to investigate the most suitable design.

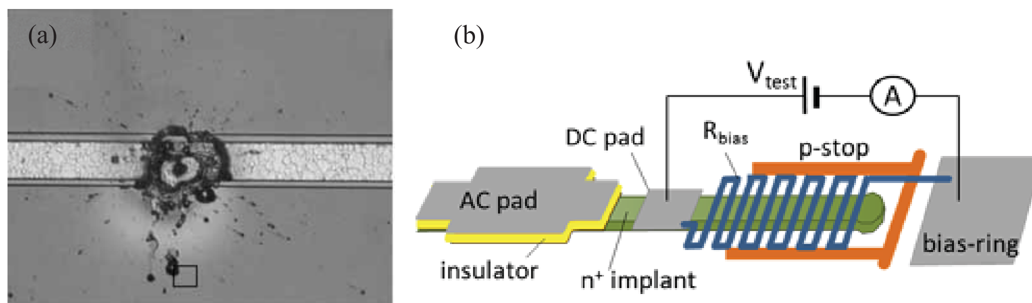

Fig. 1. (a) A hole was created on a present SCT sensor (the strip width is 22 μm) by a laser pulse equivalent to 10^8 mips. The laser was spotted in the area shown in the square. The sensor bias was 500 V; (b) Schematic drawing of the strip end for the p-bulk sensor in design. The circuit including V_{test} and an ampere-meter is used for the DC test (see text). The current generated from the beam loss is to be efficiently drained towards the bias-ring such that the implant voltage should not exceed the rating of the insulator.

2. Tested PTP Structures

In order to protect the sensor effectively, it is preferable that the punch-through occurs at low enough voltages and the impedance of the channel be low. Negative voltages are concerned on the implant strip ends against the bias-ring, since the signal current is negative in the n^+-in-p sensors. Various design issues exist for efficient PTP such as (1) the distance between the electrodes, (2) the shapes of the electrode ends, (3) the p-stop density, and (4) the gate structure above the PT region.

In the previous studies [4,5] we have discussed (2) and (3). A clear dependence on the p-stop density is observed, as explained by the p-stop functioning as a PT blocker. On the other hand, no obvious results were obtained concerning (2) for various end shapes. In fact the investigated samples were not well controlled in view of (4) the gate structure. Therefore, in this paper we systematically changed (1) the distance and (4) the gate coverage of the PT region by extending the aluminum of the bias-ring, as shown in Fig. 2. The structure Z4D3 is identical to Z4D previously studied [4,5]. The samples Z4D3, Z4D4 and Z4D5 are to be compared for the gate coverage. Z4D4 and Z4D2 are for the distance between the electrodes. For investigation of the p-stop as PT blocker, Z4D1 was added where the p-stop was excluded.

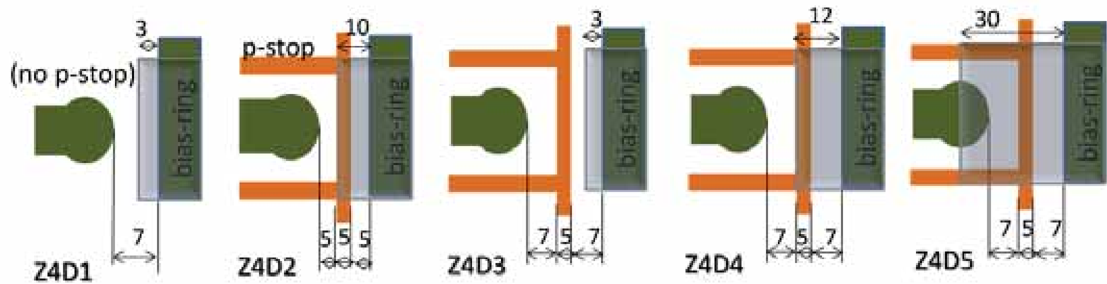

Fig. 2. Examined PTP structures (Z4D2 through D5). The "common" p-stop is 5 μm wide and floating. The overhang of the aluminum, which is DC connected to the bias-ring, is varied from 3 μm (D3), 12 μm (D4) to 30 μm (D5) to control the coverage of the PT region. Z4D2 has a distance of 5 μm between the implant end to the p-stop and between the p-stop to the bias-ring to be compared to 7 μm of Z4D4. Z4D1 is a comparison structure eliminating the p-stop.

3. Evaluation Procedures and Results

3.1. DC method

Fig. 1(b) shows the schematic diagram of the DC evaluation method of the PTP. The resistance across the DC pad and the bias-ring is measured by applying a test voltage V_{test} on the DC pad. The DC pad is located 0.5 mm from the implant strip end.

Typical resistance curves are plotted in Fig. 3(a). Since the channel is composed of $n^+(V_{test})$-p-$n^+(0V)$, the PT occurs at the implant strip end for positive and at the bias-ring for negative V_{test}. We define the PT voltage V_{PT} as V_{test} when the effective resistance is one half of the bias resistance of about 1.5 MΩ. Since the curves are not identical in shape, we also define 90% and 10% points of the bias resistance, V^-_{PT} and V^+_{PT}, respectively.

The results obtained for the test structures Z4D1 through Z4D5 are summarized in Fig. 3 where the samples are both non- and proton irradiated up to 10^{15} n_{eq}/cm^2[6]. Among these Z4D3 is the worst, showing larger V_{PT} and V^+_{PT}, while Z4D5 is the best, showing notably small V^+_{PT}. This observation

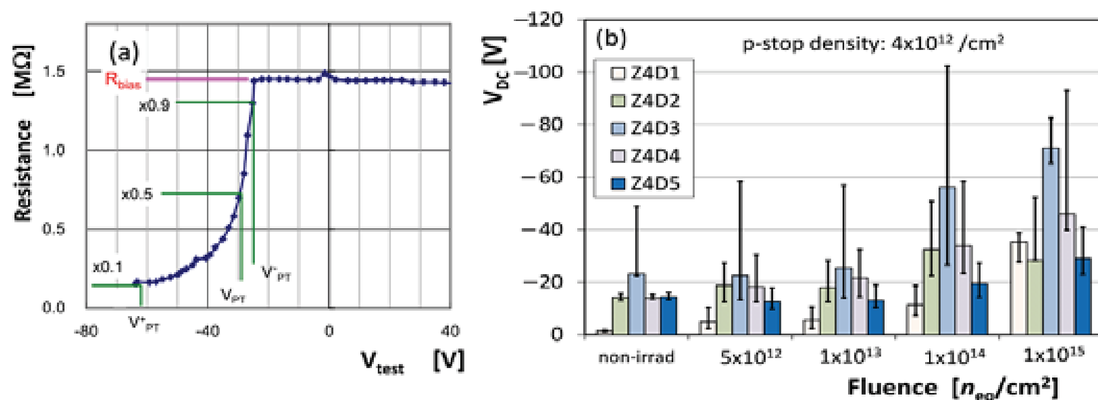

Fig. 3. (a) Examples of measured resistances as a function of V_{test}; (b) Summary of the DC results for the samples non- and proton irradiated up to 10^{15} n_{eq}/cm^2. The vertical bars represent the range of V^-_{PT} and V^+_{PT} defined in (a).

concludes the effectiveness of the gate structure that covers fully up to the strip ends where the PT occurs. The similarity between Z4D1 and Z4D5 especially at larger doses implies the effect of p-stop as a PT blocker is weakened by the gate. The sample Z4D2 having a 5 μm electrode distance is almost in agreement with Z4D4 having a 7 μm.

3.2. AC method

The DC method provides us estimates on the resistance values of the channel, while not on the time structure. We injected infrared laser pulses to simulate passage of charged particles and triggered the PT to extract the timing information.

We employed a 1064 nm Nd:YAG laser pulses with a 10 ns base width [7]. The laser intensity was tuned by adjusting the angle of a polarizer. The laser intensity expressed in terms of number of mips was calculated from the average current when the laser was pulsed at 1 kHz, assuming that a 0.32 mm thick silicon sensor produces 3.6 fC per mip. The intensity calibration is shown in Fig. 4(a). A total current of 40 μA corresponds to 1.1×10^6 mips/pulse.

The layout of the strips is sketched in Fig. 4(b). The PTP structures were implemented on one side at right. The laser focused to 10 μm square was spotted at the pre-defined locations, NEAR or FAR. The strip signals were read out from the DC pads at either ends with an oscilloscope via passive probes TEK6139B. While injecting the laser nearly at the middle of the strips, the two strip signals nearest to the injection point and one at a neighbor were read out in order to investigate the effects to neighboring strips.

Characteristic signal shapes were obtained depending on the laser injection point and readout side configurations. The two extreme cases taken for 1.1×10^6 mips/pulse are shown in Figs. 5(a) and (b) for NEAR(injection)-NEAR(readout) and FAR-FAR configurations. The quick rises (<20ns) are immediately dumped by the PTP for NEAR-NEAR, Fig. 5(a), while it takes a while for FAR-FAR, Fig. 5(b), due to the finite implant strip resistance of about 20 kΩ. In both cases, the signals rise again when the impedance changes after losing PT.

The voltages while the PT is on are plotted in Fig. 6(a). All except in FAR-FAR configuration, the stable voltage after the first peak representing the finite resistance across the PT times the current being swept away. For FAR-FAR, where the voltage gradually decreases, the maximum values are plotted. Note that below 10 μA there was no constant part representing the PT being on. Fig. 6 (b) shows the time duration while the PT is on. The duration increases linearly with the laser intensity, providing a time scale of about 2 μs for 1.1×10^6 mips/pulse.

The observed signal shapes are dependent on the impedances among the sensor electrodes and the

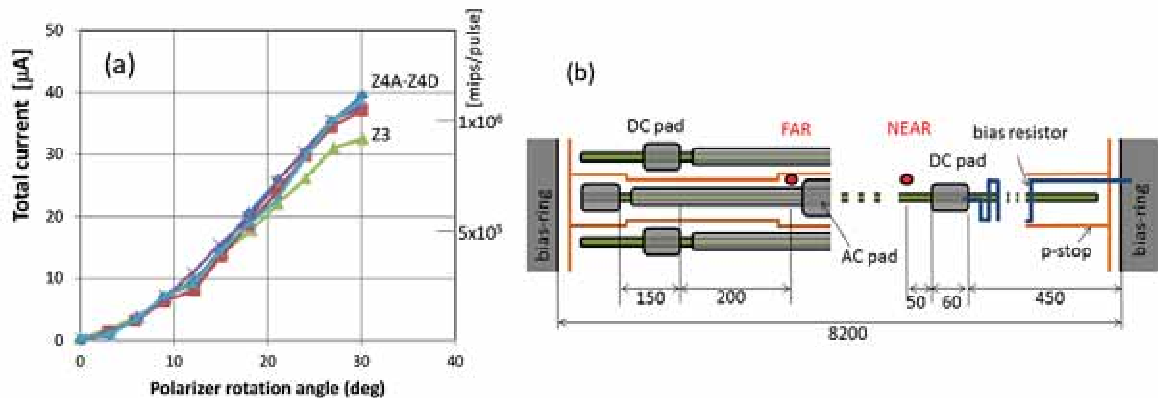

Fig. 4 (a) Total detector current as a function of the polarizer angle. The curves are shown for five different samples; (b) Diagram showing the dimensions (in μm) of test structures. The PTP structures 4D1 to Z4D5 are implemented at the right side end of the implant strip. The laser was spotted either at pre-defined NEAR or FAR positions.

readout probe, while the time information in the real case where the readout amplifier [8] is connected is concerned. The impedance of the probe is expressed as Z[MΩ]~20/*f* with frequency *f* [kHz]. Taking the amplifier impedance [8] into account, the impedance of the measurement system is about twice as that of the real case if the PT is not set. This should slow the current flow, providing almost similar voltage peaks in the two cases. The voltage is present entirely across the insulator for slower pulses (f<10MHz) or entirely across the amplifier inputs for f>100MHz. Once the PT is set, however, the impedances coincide with each other, hence the voltage and time information is presumably reproduced in this measurement.

The fast rise that appears right at laser injection is responsible for the amplifier break while the constant or slowly decaying voltages, which are summarized in Fig. 6(a), and the bump that appears after the PT is deactivated are responsible for the insulator break. As far as for the sensor, the voltages at FAR-FAR configuration are largest and are to be concerned. The probe response is linear up to 300 Vrms for f<3MHz and up to 50 Vrms for f>20MHz. This limitation for faster signals underestimates the fast signals right after the laser injection, responsible for the amplifier break.

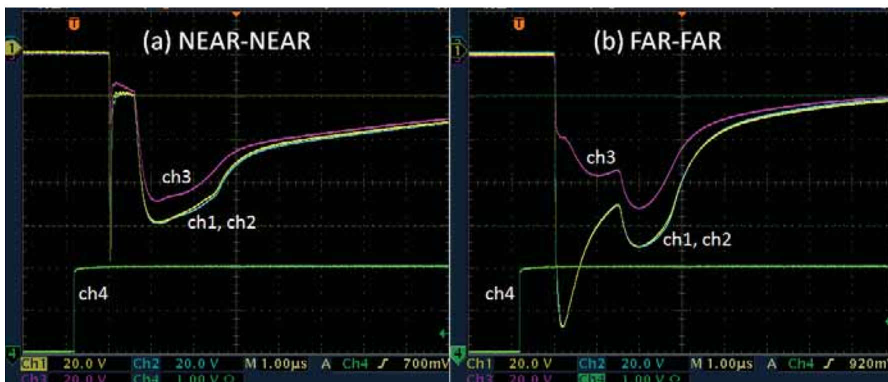

Fig. 5 Two sets of oscilloscope traces for (a) NEAR-NEAR and (b) FAR-FAR configurations for laser injection and readout positions. CH1 and CH2 are of the nearest strips to the laser injection point, CH3 is of the next neighbor. CH4 is for the laser trigger signal. Horizontal: 1 μs/div, Vertical: 20 V/div for CH1-CH3. The laser intensity was 10^6 mips/pulse with the detector bias of 200 V. The low and constant part in (a) and slowly decaying part in (b) are due to PT, the difference being described by the impedance due to the implant length. The latest bumps appear when the PT is deactivated, changing the impedance accordingly.

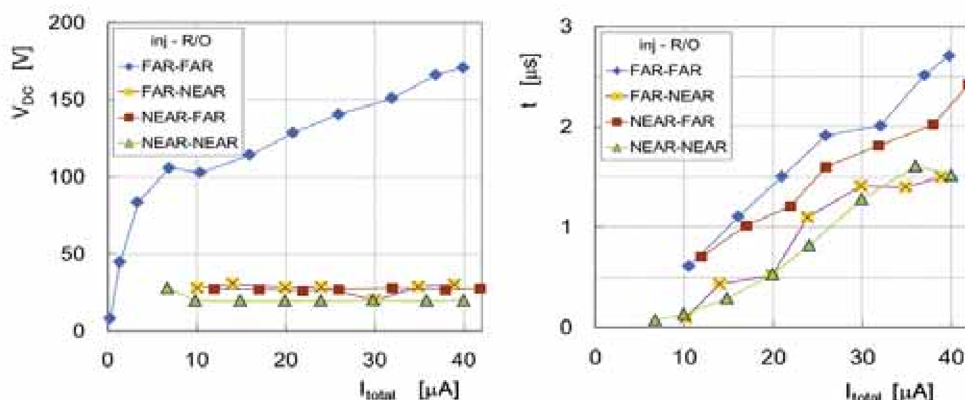

Fig. 6 (a) The voltage and (b) time while the PT is on, as a function of the detector current. The curves are for four laser injection and readout position configurations. 40 μA corresponds to 10^6 mips/pulse. The PTP structure is Z4A described in [1][2].

The voltages measured in FAR-FAR configuration are plotted in Fig. 7 for Z4D1 to Z4D5 PTP configurations in comparison with another configuration Z3 [1] where no PTP design is applied keeping a wider distance of 30 μm between the implants. The similarity of Z3 and Z4D3 (smallest gate coverage) curves suggests that the gate is more important than the separation of the electrodes for the PT to occur. The effectiveness of p-stop as the PT blocker is seen from the Z4D1 data when the gate coverage is insufficient. The Z4D5 (PT region covered entirely) is the best among the designs.

We measured also for the samples irradiated to 10^{15} n/cm^2. Since the collected charge is almost halved for the irradiated samples due to degraded charge collection, the apparent effects are smaller with respect to the laser intensity. If the curves are compared in terms of the induced current, small radiation-induced degradation was observed.

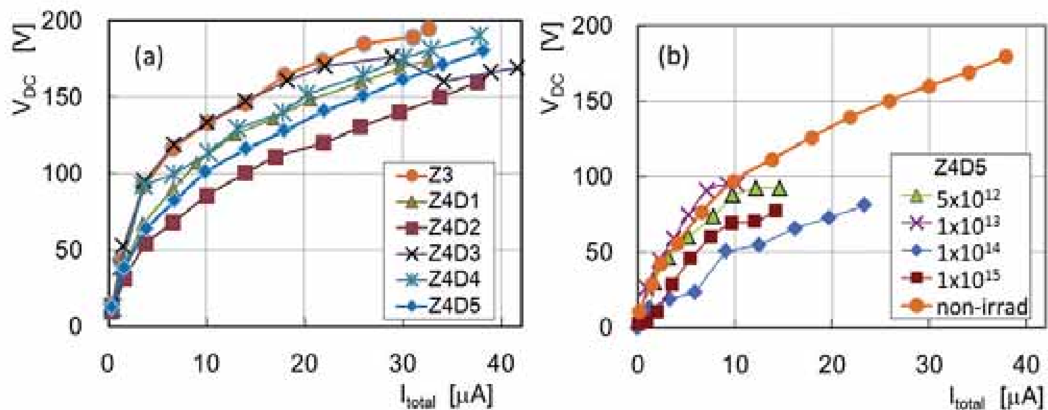

Fig. 7 Maximum voltages in FAR-FAR configuration, (a) compared among various PTP structures, (b) compared among irradiated and non irradiated Z4D5 samples. The detector was biased at 200 V.

Conclusions

The performance of various PTP designs was investigated both by DC and AC methods. We showed the effectiveness of the gate structure that suppresses the p-stop to function as a PT blocker. The finite implant resistance is most concerned, which creates a voltage difference across the strip insulator exceeding 100 V with a duration of a few μs when 1×10^6 mips/pulse is injected 8 mm from the PTP structure. The durability of the insulator against the pulses with described time structures needs to be investigated.

References

[1] Abhmad A. et al, NIM A578 (2007) 98-118.
[2] Andricek L. et al, NIM A439 (2000) 427-441.
[3] Hara K, et al., NIM A565 (2006) 538.
[4] Unno Y, et al., NIM A636 (2011) S24; Hara K, et al., NIM A636 (2011) S83 ; Lindgren, S et al., NIM A636 (2011) S111.
[5] Sadrozinski H.F.-W. et al, NIM doi:10.1016/j.nima.2011.06.085.
[6] Unno Y. et al., NIM A579 (2007) 614.
[7] Hara K. et al., NIM A541 (2005) 15.
[8] Kaplon J and Dabrowski W, IEEE TNS 52-6 (2005) 2713.